Electronic Supplementary Material (ESI) for Journal of Materials Chemistry C.

Supporting Information

Regulating the luminescence of tetraphenylethene(TPE) based lanthanide nanoparticles in the presence of organic amines/acids

Zhengyu Zhang, Jicao Han, Dongdong Liu and Xi Wang*

Marine College, Shandong University, Weihai, Weihai 264209, People's Republic of China. E-mail: xi_wang@sdu.edu.cn

Experimental

Materials and methods

The source materials used in the experiment mainly include 1-(bromomethyl) -4- (1,2,2-triphenylethenyl) benzene (Energy Chemical), pyridine (Energy Chemical), 4-methylpyridine (Energy Chemical), poly(styrene sulfonic acid) sodium salt (PSS) (Energy Chemical), europium (III) trichloride hexahydrate ($EuCl_3 \cdot 6H_2O$) (Energy Chemical), gadolinium(III) trichloride hexahydrate ($GdCl_3 \cdot 6H_2O$) (Energy Chemical), sodium orthovanadate (Na_3VO_4) (Energy Chemical), and 4,4,4-trifluoro-1-phenyl-1,3-butanedione (ABM) (Energy Chemical). These starting materials were used without further purification. The morphology of the related products were observed by TecnaiG2-20 Transmission Electron Microscope (TEM) and Regulus 8100 Scanning Electron Microscope (SEM). ^1H NMR spectra were obtained on AVANCE III HD 400 MHz Nuclear Magnetic Resonance Spectrometer. Powder X-ray diffraction (XRD) data was collected on a Rigaku Ultima IV X-ray diffractometer with Cu Kα radiation (λ = 0.15418 nm). X-ray photoelectron spectroscopy (XPS) was measured by ThermoEscalab250 spectrometer excited by monochromatic Al-Kα. Thermogravimetric analysis (TGA) was carried out on a Perkin-Elmer TGA unit in air with a heating rate of 10 K/min, and the tested products have been preliminarily dried to remove the solvents. The RT fluorescence decay curves were detected on a Edinburgh FLS980 luminoscope. UV-Vis spectra were detected on a Hitachi U-2910 Spectrophotometer. Fluorescence spectra were recorded on a Hitachi F-7000 Spectrometer. Phosphorescence spectra were done on a FS5 Spectrometer.

Synthetic procedures

Synthesis of TPE-Py. 0.2150 g of the 1-(bromomethyl)-4-(1,2,2-triphenylethenyl)benzene (TPE-Br), 0.064 mL of the pyridine, and 1.5 mL of toluene were stirred for 24 hours at room temperature. Then, the product was separated by centrifugation, washed with ether three times. The crystals of TPE-Py were obtained via vacuum drying finally.

Synthesis of TPE-Py-Me. 0.2150 g of 1-(bromomethyl)-4-(1,2,2-triphenylethenyl)benzene (TPE-Br), 0.073 mL of the 4-methylpyridine, and 1.5 mL toluene were stirred for 24 hours at room temperature. To remove the remaining reactants, the product was separated by centrifugation

and washed with ether three times. Finally, the purified solids of TPE-Py-Me were dried by vacuuming.

Preparation of TPE-Py-Me@PSS@$EuVO_4$ nanoparticles. 0.7020 g of poly(styrene sulfonic acid) sodium salt (PSS) was dissolved in 5 mL of deionized water, and 2 mL of $EuCl_3$ aqueous solution (0.25 mol/L) was added drop by drop. The mixture was stirred for 5 min and 2.50 mL of Na_3VO_4 aqueous solution (0.25 mol/L) was added into the above mixture slowly under stirring for another 5 min. Then, the mixture was transferred to Teflon-lined stainless steel autoclave (15 mL). The autoclave was placed in an oven preheated to 160 °C, and kept under static conditions for 12 h. To remove the remaining reactants, the resulting PSS@$EuVO_4$ nanoparticles was separated by centrifugation, washed with deionized water several times, and stored in a well-sealed container with 5 mL of ethanol. To modify with the TPE-motif, 1 mL of the TPE-Py-Me ethanol solution (0.50 mol/L) was dropped into the above nanoparticels and stirred at room temperature for 3h. The resulted solid was collected by centrifugation, and washed with ethanol for three times. Finally, the TPE-Py-Me@PSS@$EuVO_4$ nanoparticles were obtained and dispersed in 10 mL of ethanol.

Preparation of TPE-Py-Me@PSS/ABM@$EuVO_4$ nanoparticles. 1.002 g of 4,4,4-trifluoro-1-phenyl-1,3-butanedione (ABM) was added into the above TPE-Py-Me@PSS@$EuVO_4$ nanoaparticles suspension (10 mL of ethanol). The mixture was stirred until ABM was dissolved totally. Then, 0.1 mL of the triethylamine was added dropwise into the mixture under stirring at 50 ℃ for 3 h. The solid was collected by centrifugation and washed with ethanol for three times. The final TPE-Py-Me@PSS/ABM@$EuVO_4$ nanoparticles was obtained and dispersed in 10 mL of ethanol.

Fluorescence performance experiment. In a typical measurement of the emission spectra, certain amount of the suspension was mixed with the certain kind of solution. After ultrasonic treatment, the well-dispersed solution was added to a quartz cuvette for the measurement of its fluorescent spectrum. In the study of the luminescent response by adding amines and acid, an appropriate amount of the solution was injected. All the detection of emission spectra were generally completed within 1 min after ultrasonic treatment. In the detection of RT fluorescence decay curves, all the samples were dispersed well in pure ethanol. For TPE-Py-Me@PSS@$GdVO_4$ nanoparticles and TPE-Py-Me@PSS@$EuVO_4$ nanoparticles, the decay curves were observed at 470 nm excited at 320 nm. For TPE-Py-Me@PSS/ABM@$GdVO_4$ nanoparticles and

TPE-Py-Me@PSS/ABM@$EuVO_4$ nanoparticles, the decay curves were observed at 470 nm excited at 365 nm. The 320 nm and 365 nm filters were matched according to the above excitation wavelength, respectively. The excitation and emission monochromator slit widths were adjusted to 5.0 nm, and Time-Correlated Single Photon Counting (TCSPC) test was carried out. The related results were fitted by double exponential model, and the final result was an average of the three sets of data.

Captions

Fig. S1 Fluorescence properties of TPE-Br in ethanol/water mixture with different volume fraction of water (f_w).

Fig. S2 ^{1}H NMR spectrum of TPE-Py in $CDCl_3$.

Fig. S3 ^{1}H NMR spectrum of TPE-Py-Me in $CDCl_3$.

Fig. S4 SEM images of TPE-Py (a) and (b); SEM images of TPE-Py-Me (c) and (d).

Fig. S5 TEM images of TPE-Py-Me@PSS@$EuVO_4$ (a) and (b); TEM images of TPE-Py-Me @PSS/ABM@$EuVO_4$ nanoparticels (c) and (d).

Fig. S6 Simulated powder XRD pattern of $EuVO_4$ and experimental XRD patterns of PSS@$EuVO_4$, TPE-Py-Me@PSS@$EuVO_4$ and TPE-Py-Me@PSS/ABM@$EuVO_4$ nanoparticles.

Fig. S7 XPS survey spectra of TPE-Py-Me@PSS@$EuVO_4$ and TPE-Py-Me@PSS/ABM@$EuVO_4$ nanoparticles.

Fig. S8 FT-IR spectra of ABM, TPE-Py-Me, TPE-Py-Me@PSS@$EuVO_4$ nanoparticles and TPE-Py-Me @PSS/ABM@$EuVO_4$ nanoparticles.

Fig. S9 Thermogravimetric curves of PSS@$EuVO_4$, TPE-Py-Me@PSS@$EuVO_4$ and TPE-Py-Me @PSS/ABM@$EuVO_4$ nanoparticles.

Fig. S10 The overlapping between the emission spectrum of TPE-Py-Me and UV-vis absorption spectrum of PSS@$EuVO_4$.

Fig. S11 Fluorescence emission spectrum of PSS@$EuVO_4$ nanoparticles.

Fig. S12 Digital photos of the samples dispersed in the ethanol solution when they remain stationary from 1 to 5 mins; Tyndall effect under spotlight when they stay still after 5 mins. (A: $EuVO_4$ power without any coating ligand; S: ethanol; B: TPE-Py-Me@PSS@$EuVO_4$ nanoparticles; C: TPE-Py-Me @PSS/ABM@$EuVO_4$ nanoparticles)

Fig. S13 UV-vis absorption spectra of TPE-Py-Me@PSS@$GdVO_4$ nanoparticles(a) and PSS/ABM @$GdVO_4$ nanoparticles (b) under 77K.

Fig. S14 Phosphorescence spectra of TPE-Py-Me@PSS@$GdVO_4$ nanoparticles (a) and PSS/ABM @$GdVO_4$ nanoparticles (b) under 77K.

Fig. S15 RT fluorescence decay curves of TPE-Py-Me@PSS@$GdVO_4$ nanoparticles and TPE-Py-Me@PSS@$EuVO_4$ nanoparticles in ethanol (excited at 320 nm and observed at 470 nm).

Fig. S16 RT fluorescence decay curves of TPE-Py-Me@PSS/ABM@$GdVO_4$ nanoparticles and TPE-Py-Me@PSS/ABM@$EuVO_4$ nanoparticles in ethanol (excited at 365 nm and observed at 470 nm).

Fig. S17 Possible mechanism of the luminescence when TPE-Py-Me@PSS/ABM@$EuVO_4$ nanoparticles dispersed in ethanol/water mixed solvent with different f_w.

Fig. S18 UV-vis absorption spectra of the supernatant separated from TPE-Py-Me@PSS/ ABM@$EuVO_4$ nanoparticles when water fraction (f_w) increased to 50% compared with TPE-Py-Me@PSS/ ABM@$EuVO_4$ nanoparticles and ABM.

Fig. S19 Emission spectra of TPE-Py-Me@PSS@$EuVO_4$ nanoparticles, TPE-Py-Me@PSS@$EuVO_4$ nanoparticles with addition of aniline, PSS @$EuVO_4$ nanoparticles with addition of aniline, TPE-Py-Me with addition of aniline and pure aniline (1 mol/L) in ethanol solution (λex= 320 nm).

Fig. S20 Possible coordination modes of Eu^{3+}-citric acid complex and Eu^{3+}-malonic acid complexes.

Fig. S21 UV-vis absorption spectra of TPE-Py-Me@PSS/ABM@$EuVO_4$ nanoparticles, TPE-Py-Me@PSS/citric acid@$EuVO_4$ nanoparticles, TPE-Py-Me@PSS/ABM@$EuVO_4$ nanoparticles-citric acid, citric acid, and ABM (concentration of citric acid: 5.0×10^{-4} moL/L).

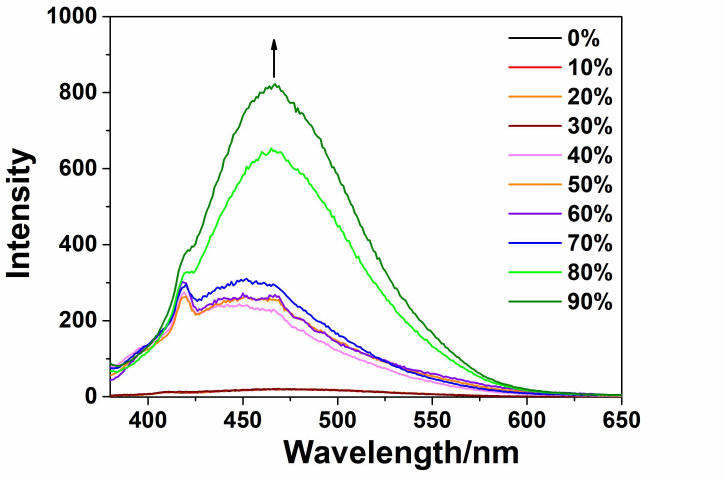

Fig S1. Fluorescence properties of TPE-Br in ethanol/water mixture with different volume fraction of water (f_w).

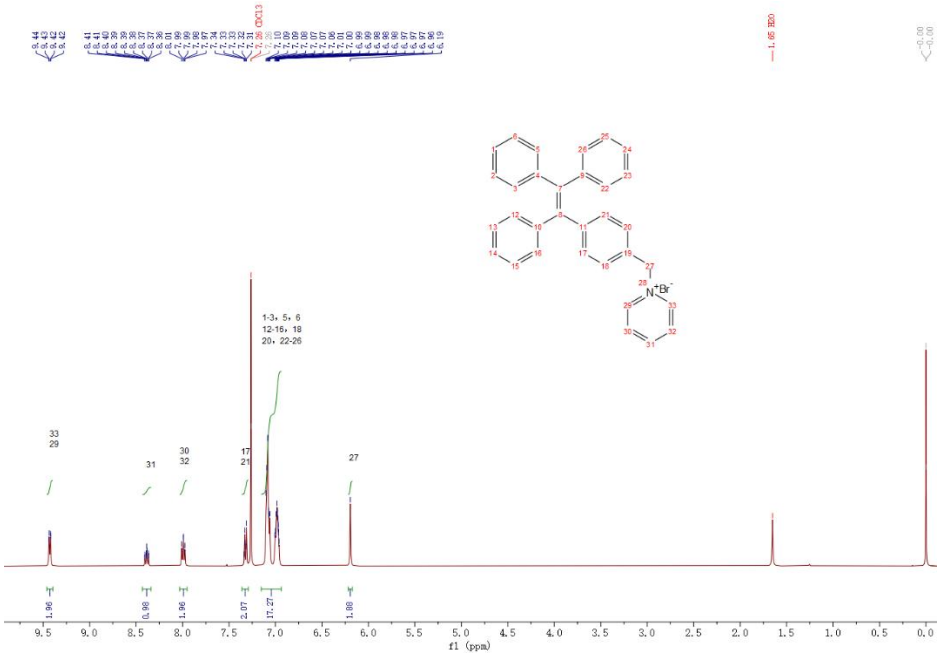

Fig S2. ^{1}H NMR spectrum of TPE-Py in $CDCl_3$.

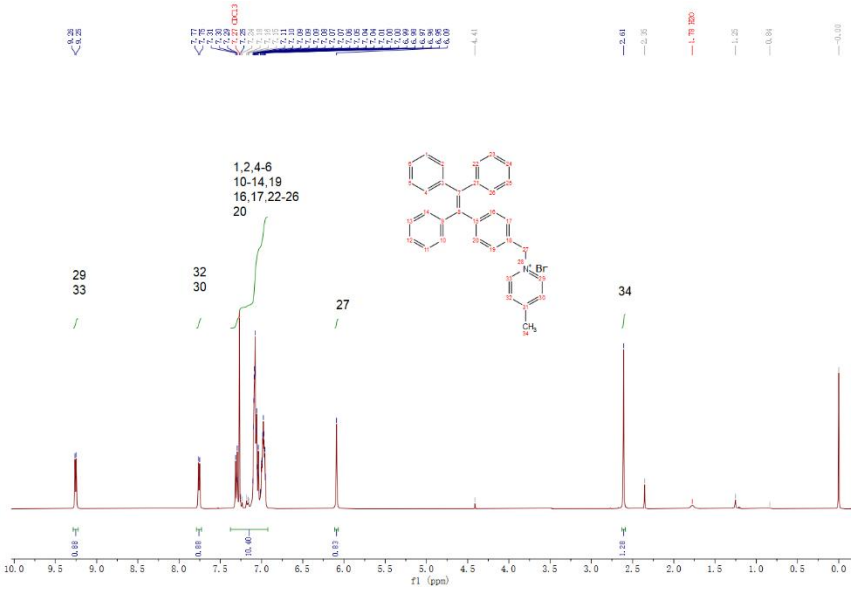

Fig S3. ^{1}H NMR spectrum of TPE-Py-Me in $CDCl_3$.

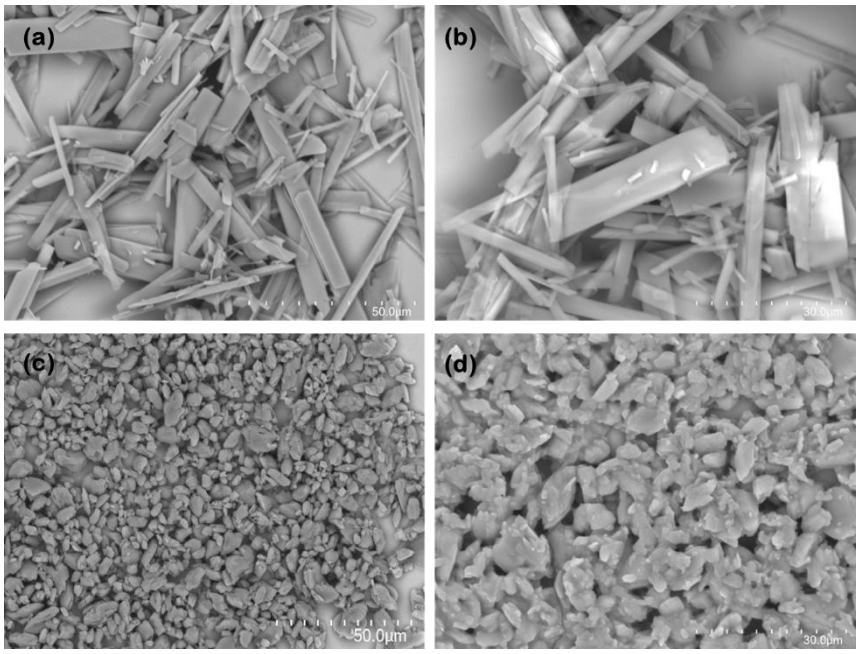

Fig S4. SEM images of TPE-Py (a) and (b); SEM images of TPE-Py-Me (c) and (d).

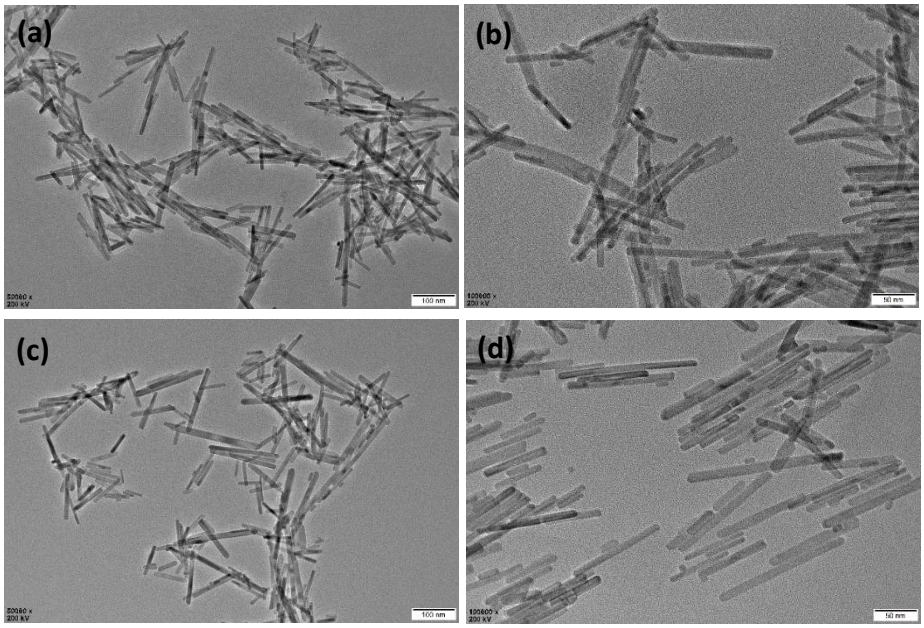

Fig. S5 TEM images of TPE-Py-Me@PSS@$EuVO_4$ (a) and (b); TEM images of TPE-Py-Me @PSS/ABM@$EuVO_4$ nanoparticels (c) and (d).

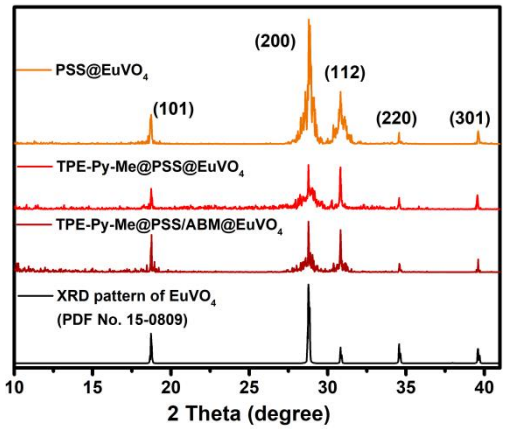

Fig. S6 Simulated powder XRD pattern of $EuVO_4$ and experimental XRD patterns of PSS@$EuVO_4$, TPE-Py-Me@PSS@$EuVO_4$ and TPE-Py-Me@PSS/ABM@$EuVO_4$ nanoparticles.

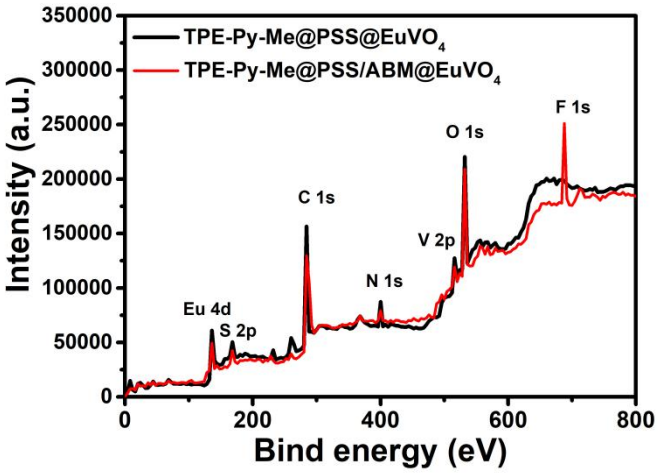

Fig. S7 XPS survey spectra of TPE-Py-Me@PSS@$EuVO_4$ and TPE-Py-Me @PSS/ABM@$EuVO_4$ nanoparticles.

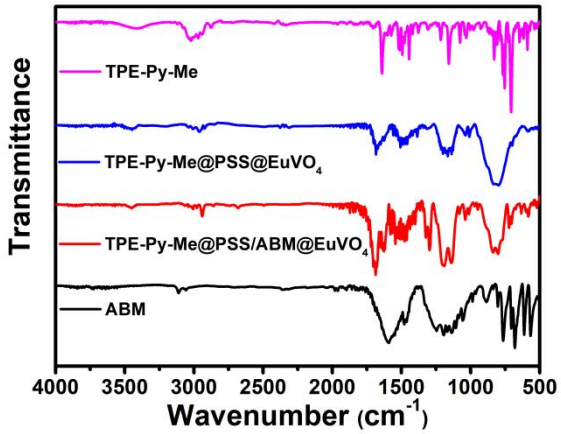

Fig. S8 FT-IR spectra of ABM, TPE-Py-Me, TPE-Py-Me@PSS@$EuVO_4$ nanoparticles and TPE-Py-Me @PSS/ABM@$EuVO_4$ nanoparticles.

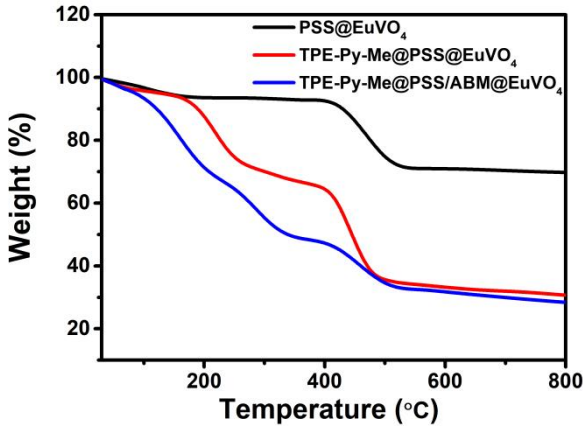

Fig. S9 Thermogravimetric curves of PSS@$EuVO_4$, TPE-Py-Me@PSS@$EuVO_4$ and TPE-Py-Me @PSS/ABM@$EuVO_4$ nanoparticles.

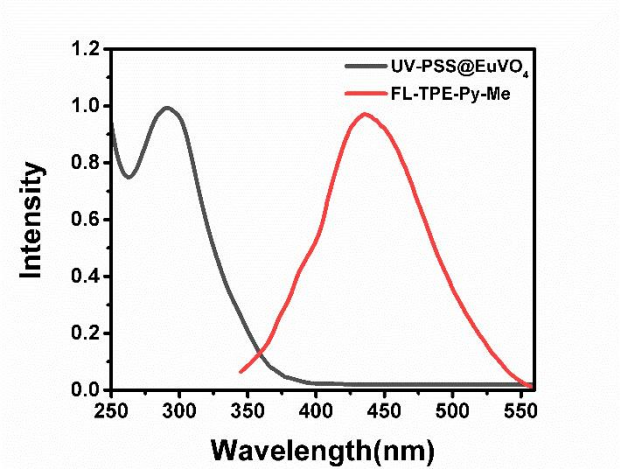

Fig. S10 The overlapping between the emission spectrum of TPE-Py-Me and UV-vis absorption spectrum of PSS@$EuVO_4$.

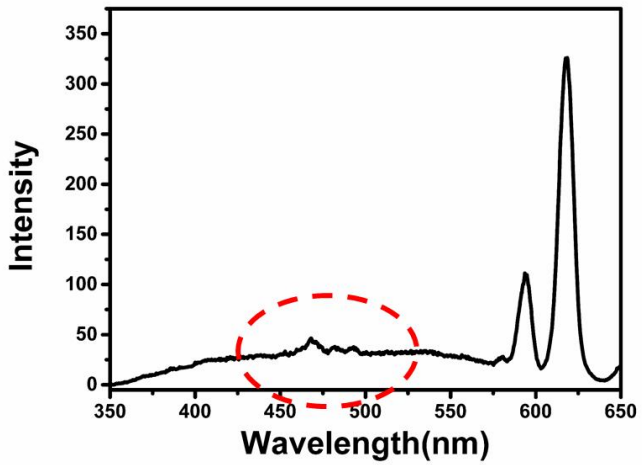

Fig. S11 Fluorescence emission spectrum of PSS@$EuVO_4$ nanoparticles.

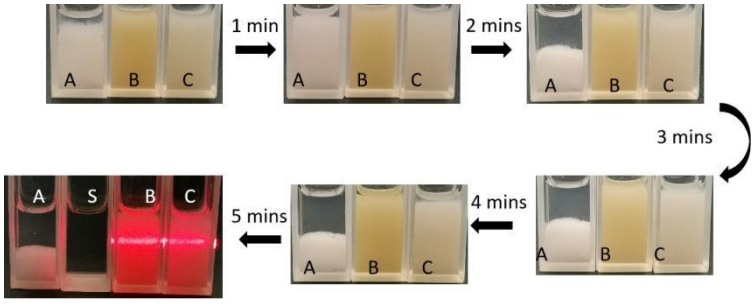

Fig. S12 Digital photos of the samples dispersed in the ethanol solution when they remain stationary from 1 to 5 mins; Tyndall effect under spotlight when they stay still after 5 mins. (A: $EuVO_4$ power without any coating ligand; S:ethanol; B: TPE-Py-Me@PSS@$EuVO_4$ nanoparticles; C: TPE-Py-Me @PSS/ABM@$EuVO_4$ nanoparticles)

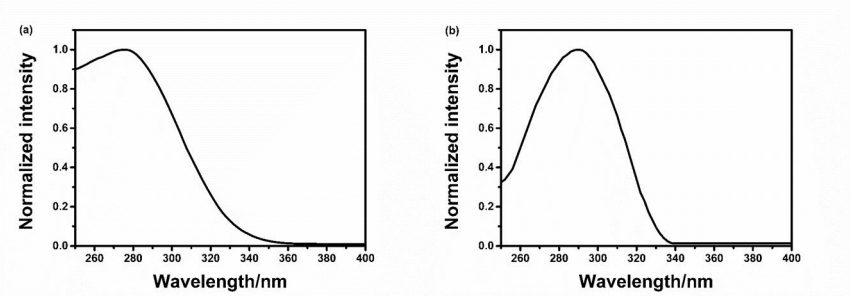

Fig. S13 UV-vis absorption spectra of TPE-Py-Me@PSS@$GdVO_4$ nanoparticles(a) and PSS/ABM @$GdVO_4$ nanoparticles (b) under 77K.

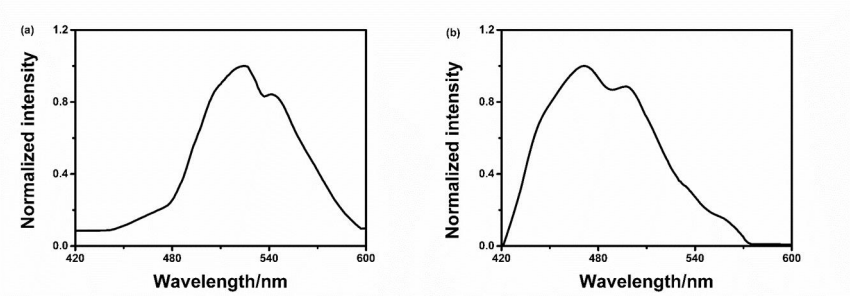

Fig. S14 Phosphorescence spectra of TPE-Py-Me@PSS@$GdVO_4$ nanoparticles(a) and PSS/ABM @$GdVO_4$ nanoparticles (b) under 77K.

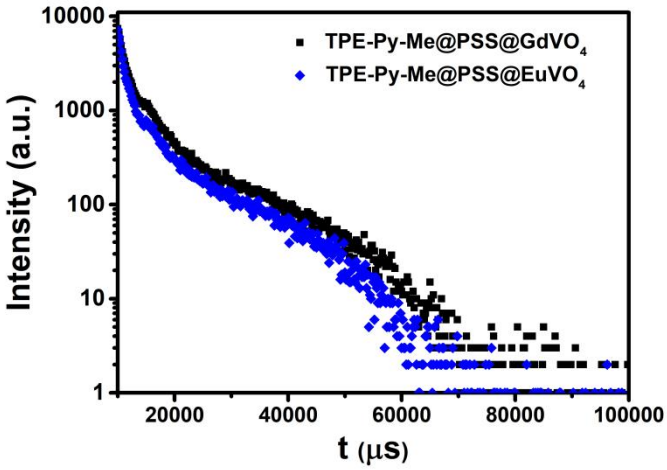

Compounds	τ_1 (μs)	A_1	τ_2 (μs)	A_2	τ (μs)
TPE-Py-Me@PSS@$GdVO_4$	1.4301	10088.03	10.9981	1242.02	6.085
TPE-Py-Me@PSS @$EuVO_4$	1.2493	12132.09	10.3622	939.21	4.813

Fitting curve formula $R(t)=A_0+A_1e^{(-t/\tau 1)}+A_2e^{(-t/\tau 2)}$

$\tau=\frac{\tau_1^2A_1+\tau_2^2A_2}{\tau_1A_1+\tau_2A_2}$ τ_1 is fast decay time and τ_2 is slow decay time.

Fig. S15 RT fluorescence decay curves of TPE-Py-Me@PSS@$GdVO_4$ nanoparticles and TPE-Py-Me@PSS@$EuVO_4$ nanoparticles in ethanol (excited at 320 nm and observed at 470 nm).

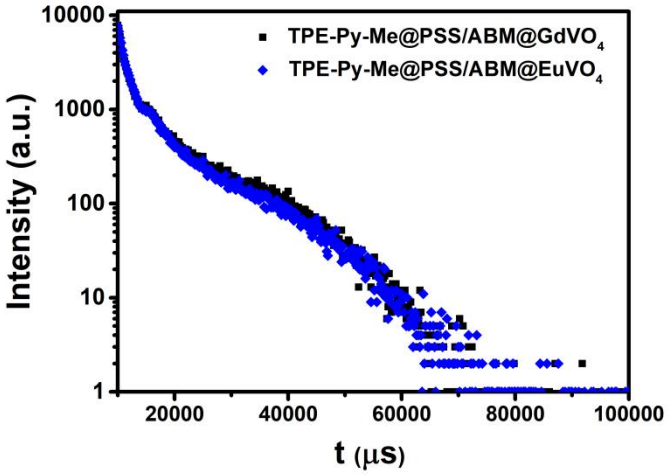

Compounds	τ_1 (μs)	A_1	τ_2 (μs)	A_2	τ (μs)
TPE-Py-Me@PSS/ABM@$GdVO_4$	1.3664	11609.12	10.8083	1348.56	5.887
TPE-Py-Me@PSS/ABM@$EuVO_4$	1.4426	11467.62	10.4487	1251.23	5.418

Fitting curve formula $R(t)=A_0+A_1e^{(-t/\tau 1)}+A_2e^{(-t/\tau 2)}$

$\tau=\frac{\tau_1^2A_1+\tau_2^2A_2}{\tau_1A_1+\tau_2A_2}$ τ_1 is fast decay time and τ_2 is slow decay time.

Fig. S16 RT fluorescence decay curves of TPE-Py-Me@PSS/ABM@$GdVO_4$ nanoparticles and TPE-Py-Me@PSS/ABM@$EuVO_4$ nanoparticles in ethanol (excited at 365 nm and observed at 470 nm).

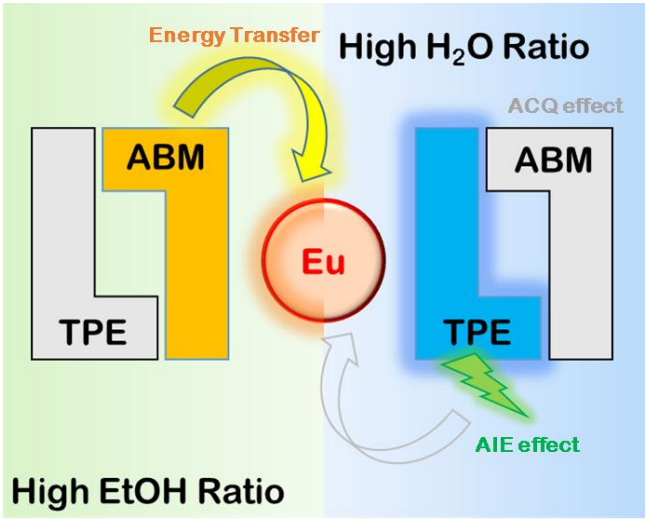

Fig. S17 Possible mechanism of the luminescence when TPE-Py-Me@PSS/ABM@$EuVO_4$ nanoparticles dispersed in ethanol/water mixed solvent with different f_w.

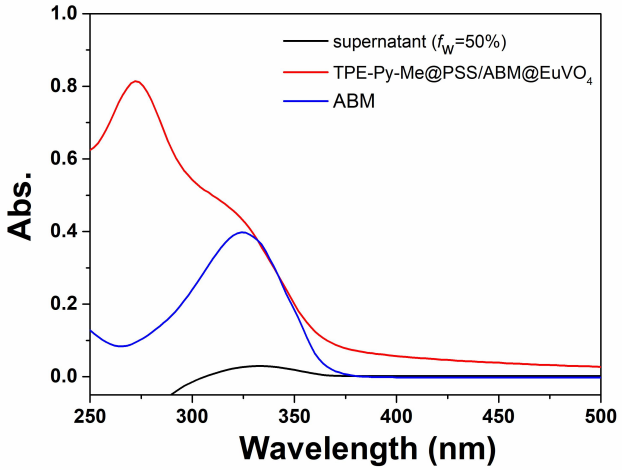

Fig. S18 UV-vis absorption spectra of the supernatant separated from TPE-Py-Me@PSS/ ABM@$EuVO_4$ nanoparticles when water fraction (f_w) increased to 50% compared with TPE-Py-Me@PSS/ ABM@$EuVO_4$ nanoparticles and ABM.

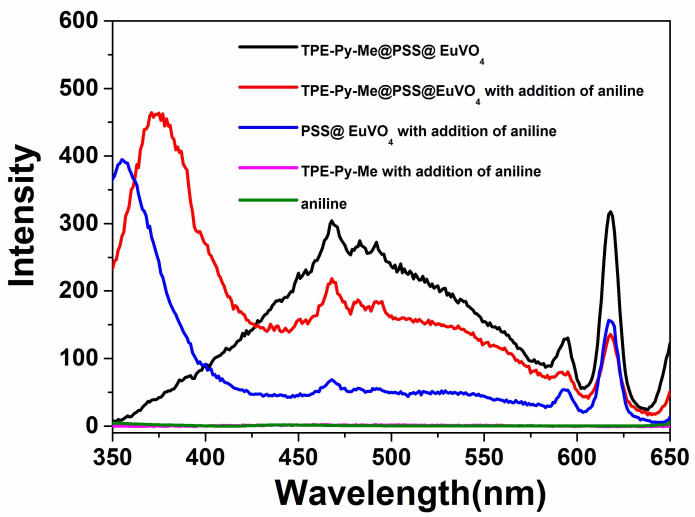

Fig. S19 Emission spectra of TPE-Py-Me@PSS@$EuVO_4$ nanoparticles, TPE-Py-Me@PSS@$EuVO_4$ nanoparticles with addition of aniline, PSS @$EuVO_4$ nanoparticles with addition of aniline, TPE-Py-Me with addition of aniline and pure aniline (1 mol/L) in ethanol solution (λex= 320 nm).

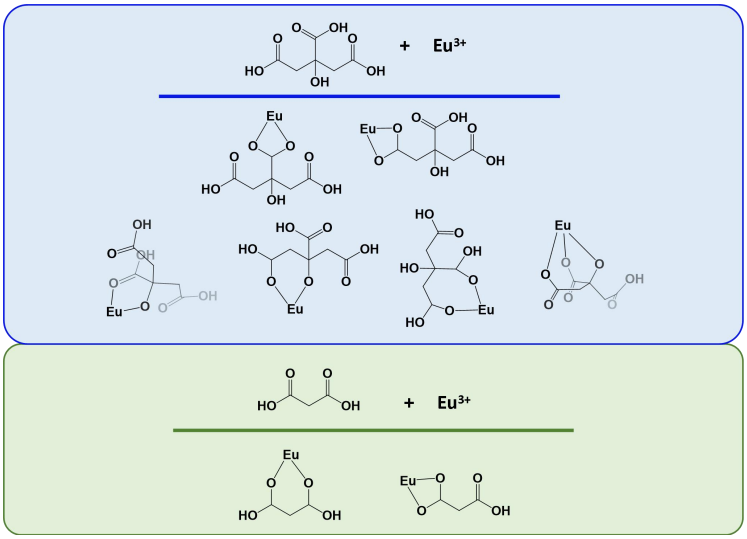

Fig. S20 Possible coordination modes of Eu^{3+}-citric acid complex and Eu^{3+}-malonic acid complexes.

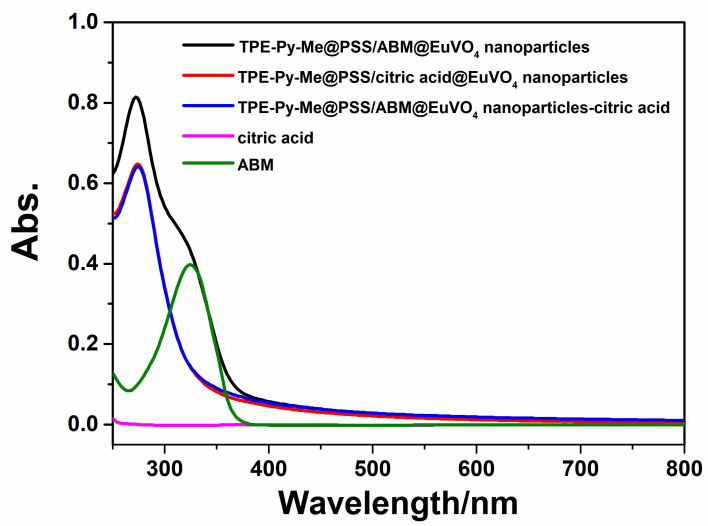

Fig. S21 UV-vis absorption spectra of TPE-Py-Me@PSS/ABM@$EuVO_4$ nanoparticles, TPE-Py-Me@PSS/citric acid@$EuVO_4$ nanoparticles, TPE-Py-Me@PSS/ABM@$EuVO_4$ nanoparticles-citric acid, citric acid, and ABM (concentration of citric acid: 5.0×10^{-4} moL/L).

Table S1 Summary of FT-IR spectra in ABM, TPE-Py-Me, TPE-Py-Me@PSS@$EuVO_4$ nanoparticles and TPE-Py-Me @PSS/ABM@$EuVO_4$ nanoparticles.

Compounds	ν(Ar-H)(cm^{-1})	ν(C=N)(cm^{-1})	ν(C=C)(cm^{-1})	ν(C=O)(cm^{-1})	ν(C-F)(cm^{-1})
TPE-Py-Me	3020	1626	1493	/	/
ABM	3059	/	/	1598	1280
TPE-Py-Me@PSS@$EuVO_4$	3008	1624	1490	/	/
TPE-Py-Me@PSS/ABM@$EuVO_4$	3005	1626	1491	1578	1294

Table S2 Summary of TGA in TPE-Py-Me@PSS@$EuVO_4$ and TPE-Py-Me @PSS/ABM@$EuVO_4$ nanoparticles.

Compounds	Reduced Mass (30-400℃)	Reduced Mass(400-800℃)
TPE-Py-Me@PSS@$EuVO_4$	34.97 %	33.79 %
TPE-Py-Me@PSS/ABM@$EuVO_4$	52.24%	18.91%